

Dielectric elastomer cylindrical actuators: electromechanical modelling and experimental evaluation

Federico Carpi*, Danilo De Rossi

Interdepartmental Research Centre "E. Piaggio", Faculty of Engineering, University of Pisa, via Diotisalvi, 2-56100 Pisa, Italy

Accepted 13 February 2004

Available online 12 April 2004

Abstract

This paper presents an experimentally validated electromechanical model of cylindrical actuators made of dielectric elastomers with compliant electrodes. Modelling was based on independent electrical and mechanical analyses of the specific configuration of the device. The expressions of the electrostatic pressures exerted by the electrodes in response to an applied voltage were formulated and inserted into the expressions of the actuator mechanical deformations, obtained by assuming linearly elastic stress–strain constitutive equations of the material for small strains. Values of axial strains expected from the model well fit those recorded from a realised actuator, electrically stimulated by step-wise high voltages. This actuator has carbon grease electrodes smeared on a cylinder-shaped silicone elastomer, showing a room-temperature-relative dielectric constant of 3 within a wide frequency range (10–10⁹ Hz). An axial strain of 4.5% due to a voltage per unit wall thickness of 100 V/μm was measured at a 5% axial prestrain, around which the material held a Young's modulus of 5 MPa.

© 2004 Elsevier B.V. All rights reserved.

Keywords: Dielectric elastomer; Cylindrical actuator; Tube actuator; Electromechanical modelling

1. Introduction

The actuating performances of elastomeric dielectric materials, used as electromechanical polymer transducers, have been assessed and continuously improved during the last few years, so that devices made of dielectric elastomers represent today one of the best technologies for polymer actuation [1–6].

Besides improving material properties and device configuration, modelling is a useful step for the development of a new actuator, enabling its rational and reliable engineering design. On this regard, this study proposes an electromechanical model and presents experimental results concerning the active deformations of a dielectric elastomer actuator having a cylindrical configuration.

This kind of device was proposed for the first time by Pelrine et al. [1], who called it *tube* actuator. It consists of a thin-walled cylindrical tube of a dielectric elastomer, having two compliant electrodes on the internal and external lateral surfaces (Fig. 1a). By applying a voltage between the

compliant electrodes, the interposed tube wall is squeezed, causing an axial elongation (Fig. 1b).

Following the electromechanical testing of a silicone-made cylindrical actuator, an experimental validation of the proposed electromechanical model is presented in this paper: the active axial strains of the tested device, measured for different applied voltages, are compared to the corresponding values expected from the developed model.

2. Materials and methods

2.1. Electromechanical modelling: general principles

The electromechanical modelling, aimed at the determination of analytical relations between the applied voltage and the resulting active strains, was based on the following simplifying assumption: the electrostatic pressures exerted by the electrodes are considered to be constant during actuation. This permits to write such pressures in terms of the geometrical dimensions held by the device only at the beginning of actuation. The related degree of approximation of modelling results was accepted in consideration of the

* Corresponding author. Tel.: +39-00-554134; fax: +39-00-550650.
E-mail address: f.carpi@ing.unipi.it (F. Carpi).

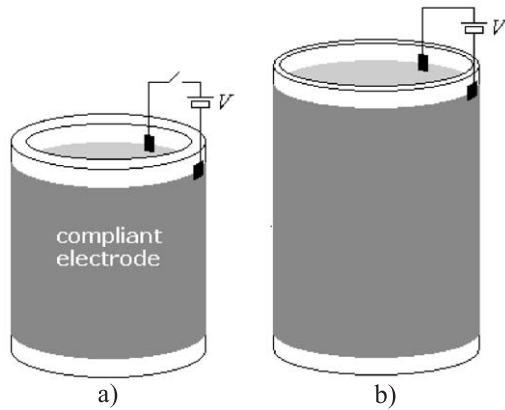


Fig. 1. Perspective view of a dielectric elastomer cylindrical (*tube*) actuator on its rest (a) and electrically activated (b) conditions.

relatively limited strain range within which the model was evaluated (Section 3.4).

Following this assumption, the electromechanical model was derived by performing two kinds of independent theoretical analyses, described below, of the actuator configuration.

A purely electrical analysis enabled the definition of the expressions of the electrostatic pressures exerted by the electrically charged electrodes, calculated as the modulus of the gradient (divided by the two electrode areas) of the electrostatic energy stored by the actuator. This methodological approach was the same adopted by Pelrine et al. [1] to deduce the electrostatic pressure p acting on a dielectric elastomer planar actuator of thickness d , subjected to a voltage V :

$$p = \varepsilon \left(\frac{V}{d} \right)^2 \quad (1)$$

where

$$\varepsilon = \varepsilon_r \varepsilon_0 \quad (2)$$

being ε_r the relative dielectric constant of the elastomer and ε_0 the dielectric permittivity of vacuum ($\varepsilon_0 = 8.85 \times 10^{-12}$ F/m).

A purely mechanical analysis, based on assumed linearly elastic properties of the elastomer for small strains, led to the relations describing the active stresses and strains, as functions of two generic pressures applied to the internal and external cylindrical surfaces.

Finally, the combination of the results of the two different kinds of investigation mentioned above gave the equations quantifying the electromechanical transduction.

2.2. Actuator realisation

A commercial silicone (poly(dimethylsiloxane)) tubing (Detakta, Germany, 01502 type), having a rest external radius of 1 mm and a rest wall thickness of 0.2 mm, was used to realise a cylindrical actuator, in order to validate the

model. Fifty-millimeter-long samples were cut from the tubing and carbon conductive grease (Tecnolube Seal, USA, Nyogel 755G) was smeared on the internal and external surfaces, so that to realise the compliant electrodes. The electrode length was made smaller than that of the entire device (Fig. 1), so that to avoid the risk of short circuit between the electrodes.

2.3. Material characterisation

The Young's modulus and relative dielectric constant of the silicone elastomer represent input parameters of the model, describing the material in use, as it will be shown by the equations presented in Sections 3.1 and 3.2. In order to measure these quantities, mechanical and dielectric characterisation of the used silicone was performed.

In particular, the passive stress–strain characteristic resulting from a test of uniaxial extension was determined, by applying increasing forces and by detecting the related strains, up to a strain of 145%.

Furthermore, the real and imaginary parts of the complex relative dielectric constant of the unstrained material were measured in the frequency range 10 – 10^9 Hz, by means of a coaxial cylindrical capacitor cell, connected to a vector network analyser (Rohde and Schwarz, Germany, ZVRE). The dielectric parameters of the sample were calculated by following the procedure reported in Ref. [7].

Both mechanical and dielectric measurements were made at a room temperature of 25 °C.

2.4. Actuator electromechanical testing

Electrically induced axial strains of the realised actuator were measured by placing the device in vertical position, with its lower end constrained and its upper end connected to an isotonic displacement transducer (Ugo Basile, Italy, 7006) (Fig. 2). This transducer also exerted a definite axial prestress on the actuator, corresponding to a 5% axial prestrain. Such a low prestrain value was chosen to consent a reasonable comparison between experimental data and modelling results, owing to the small-strains operative range implied by the assumed linearly elastic schematisation of the material.

Values of the inner and outer radii of the axially prestrained actuator were easily calculated, by using the same

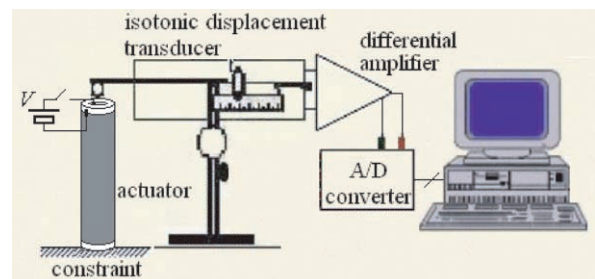


Fig. 2. Experimental set-up for measurement of isotonic axial strain.

method followed for planar actuators by Pelrine et al. [1]. This simple procedure, described below, takes advantage of the property of constancy of volume (elastomer incompressibility), which holds true for most of rubber-like materials [8], as those considered in this study. Let us indicate with a_r , b_r and L_r the rest (unstrained) inner radius, outer radius and electrode length, respectively, of the actuator and with a , b and L the corresponding prestrained dimensions. The property of volume conservation from the unstrained to a prestrained state is expressed by the following relation:

$$\pi(b^2 - a^2)L = \pi(b_r^2 - a_r^2)L_r \quad (3)$$

This equation can be written also in terms of the percentage variation of each geometrical dimension from the unstrained to the prestrained value, with respect to the unstrained one:

$$\left[b_r^2 \left(1 + \frac{b - b_r}{b_r} \right)^2 - a_r^2 \left(1 + \frac{a - a_r}{a_r} \right)^2 \right] L_r \left(1 + \frac{L - L_r}{L_r} \right) = (b_r^2 - a_r^2)L_r \quad (4)$$

where $(L - L_r)/L_r = 5\%$. Furthermore, the percentage variation of the inner and outer radii can be assumed as equal, by symmetry, since prestress is applied along the axial direction only:

$$\frac{b - b_r}{b_r} = \frac{a - a_r}{a_r} \quad (5)$$

Consequently, Eq. (4) becomes:

$$\left(1 + \frac{b - b_r}{b_r} \right)^2 \left(1 + \frac{L - L_r}{L_r} \right) = 1 \quad (6)$$

which admits this solution:

$$\frac{b - b_r}{b_r} = -1 + \frac{1}{\sqrt{1 + \frac{L - L_r}{L_r}}} \quad (7)$$

Eqs. (5) and (7) enable the calculation of the prestrained radii, resulting from the imposed 5% axial prestrain: $a = 0.781$ mm ($a_r = 0.8$ mm), $b = 0.976$ mm ($b_r = 1$ mm), corresponding to a wall thickness of $b - a = 0.195$ mm.

In this prestrained condition, step-wise voltages of different value, generated by a DC high-voltage supply (Bertan, USA, HV-DC 205A-30P), were separately applied to the actuator and 10-s duration signals of occurring isotonic axial displacement were successively recorded for each voltage value.

3. Results

3.1. Electrical modelling

The goal of the electrical modelling of the actuator is the derivation of the expressions of the electrostatic pressures

exerted by the compliant electrodes, when a voltage is applied between them.

Before the application of the two radial pressures, the actuator is assumed at mechanical equilibrium. In this condition, a resulting generic inner radius a , outer radius b and electrode length L are considered, regardless of the actual value of the axial prestress (which could also be null, at worst, for the aim of the present section), balanced by the related material recovery stress.

The elastomeric actuator with hollow cylindrical shape can be electrically modelled as a compliant cylindrical capacitor, geometrically defined by the extension of the device electrodes and having electrical capacitance

$$C = \frac{2\pi\epsilon L}{\ln\left(\frac{b}{a}\right)} \quad (8)$$

The elastomer is here supposed as isotropic and its dielectric constant is assumed not to vary with the stress or strain state of the material, nor with the applied electric field.

The electrostatic pressures p_a and p_b , exerted by the internal and external electrodes, respectively, in response to an applied voltage V (Fig. 3), are expressed by the modulus F of the electrostatic force acting between the electrodes, divided by their area. F can be obtained as the modulus of the gradient of the electrostatic energy U stored by the actuator, leading to the following expressions:

$$p_a = \frac{F}{2\pi a L} = \frac{|\nabla U|}{2\pi a L} \quad (9)$$

$$p_b = \frac{F}{2\pi b L} = \frac{|\nabla U|}{2\pi b L} \quad (10)$$

where

$$U = \frac{1}{2} C V^2 = \frac{\pi\epsilon L V^2}{\ln\left(\frac{b}{a}\right)} \quad (11)$$

Since the compliance of the actuator, U is a function of the three geometrical variables a , b and L , for each definite

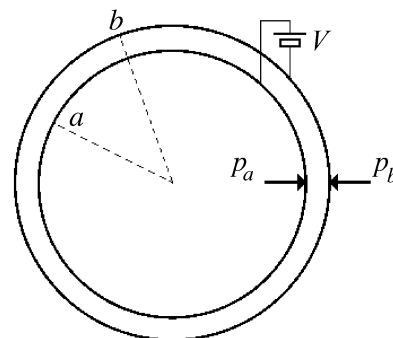


Fig. 3. Actuator top view.

value of the applied voltage (assumed constant during actuation). Consequently, the derivation of $|\nabla U|$ would require, in principle, this calculation:

$$|\nabla U| = \sqrt{\left(\frac{\partial U}{\partial a}\right)^2 + \left(\frac{\partial U}{\partial b}\right)^2 + \left(\frac{\partial U}{\partial L}\right)^2} \quad (12)$$

However, the material incompressibility gives a further relation among the three variables, allowing to express $|\nabla U|$ as a function of only two of them, as we describe below.

Let us consider the differential of U :

$$dU = \frac{\partial U}{\partial a} da + \frac{\partial U}{\partial b} db + \frac{\partial U}{\partial L} dL \quad (13)$$

and the partial derivatives

$$\frac{\partial U}{\partial a} = \frac{\pi \varepsilon L V^2}{a \ln^2\left(\frac{b}{a}\right)} \quad (14)$$

$$\frac{\partial U}{\partial b} = -\frac{\pi \varepsilon L V^2}{b \ln^2\left(\frac{b}{a}\right)} \quad (15)$$

$$\frac{\partial U}{\partial L} = \frac{\pi \varepsilon V^2}{\ln\left(\frac{b}{a}\right)} \quad (16)$$

The property of constancy of volume ($\text{Vol}=k=\text{constant}$) can be translated in this condition:

$$d(\text{Vol}) = 0 \Rightarrow d(\pi(b^2 - a^2)L) = 0 \quad (17)$$

which leads to this relation among da , db and dL :

$$dL = \frac{2L(ada - bdb)}{b^2 - a^2} \quad (18)$$

Through the combination of Eqs. (13)–(16) with Eq. (18), dU can be written as a function of da and db only:

$$dU = \frac{\partial U}{\partial a} \Big|_{\text{Vol}=k} da + \frac{\partial U}{\partial b} \Big|_{\text{Vol}=k} db \quad (19)$$

where

$$\frac{\partial U}{\partial a} \Big|_{\text{Vol}=k} = \frac{\pi \varepsilon L V^2}{\ln^2\left(\frac{b}{a}\right)} \frac{\left(b^2 - a^2 + 2a^2 \ln\left(\frac{b}{a}\right)\right)}{a(b^2 - a^2)} \quad (20)$$

$$\frac{\partial U}{\partial b} \Big|_{\text{Vol}=k} = -\frac{\pi \varepsilon L V^2}{\ln^2\left(\frac{b}{a}\right)} \frac{\left(b^2 - a^2 + 2b^2 \ln\left(\frac{b}{a}\right)\right)}{b(b^2 - a^2)} \quad (21)$$

This means that $|\nabla U|$ can be calculated as:

$$|\nabla U| = \sqrt{\left(\frac{\partial U}{\partial a} \Big|_{\text{Vol}=k}\right)^2 + \left(\frac{\partial U}{\partial b} \Big|_{\text{Vol}=k}\right)^2} \quad (22)$$

Finally, Eqs. (9) and (10) combined with Eqs. (20)–(22) give Eqs. (23) and (24), representing the expressions of the pressures p_a and p_b .

$$p_a = \frac{\varepsilon V^2}{2 \ln^2\left(\frac{b}{a}\right) a^2 b (b^2 - a^2)} \times \sqrt{a^6 + b^6 - a^2 b^4 - b^2 a^4 + 8 \ln\left(\frac{b}{a}\right) (b^2 - a^2) a^2 b^2 + 4 \ln^2\left(\frac{b}{a}\right) (b^2 + a^2) a^2 b^2} \quad (23)$$

$$p_b = \frac{\varepsilon V^2}{2 \ln^2\left(\frac{b}{a}\right) a b^2 (b^2 - a^2)} \times \sqrt{a^6 + b^6 - a^2 b^4 - b^2 a^4 + 8 \ln\left(\frac{b}{a}\right) (b^2 - a^2) a^2 b^2 + 4 \ln^2\left(\frac{b}{a}\right) (b^2 + a^2) a^2 b^2} \quad (24)$$

3.2. Mechanical modelling

In order to derive the relations expressing the stresses and strains produced by two generic pressures p_a and p_b (regardless of the origin of such pressures), exerted on the portions of the internal and external cylindrical surfaces corresponding to the electrode extensions, a mechanical analysis of the device was carried out, modelling the elastomer, for small strains, as a linearly elastic, isotropic and homogeneous body.

Consistently to Section 3.1, the actuator not yet stressed by the radial pressures is assumed to hold an equilibrium state, characterised by a resulting generic inner radius a , outer radius b and electrode length L .

The pressure-induced strains of the actuator can be obtained after the identification of the related displacements. This can be done by using the Navier's equations for displacements [9]. For time-invariant displacements (static condition) and in the absence of body forces per unit mass (such as gravity), the Navier's equations in cylindrical coordinates r , θ , z are [9]:

$$(\lambda + \mu) \frac{\partial}{\partial r} \left(\frac{1}{r} \frac{\partial}{\partial r} (r u_r) + \frac{1}{r} \frac{\partial u_\theta}{\partial \theta} + \frac{\partial u_z}{\partial z} \right) + \mu \left(\frac{\partial^2 u_r}{\partial r^2} + \frac{1}{r} \frac{\partial u_r}{\partial r} + \frac{1}{r^2} \frac{\partial^2 u_r}{\partial \theta^2} + \frac{\partial^2 u_r}{\partial z^2} - \frac{u_r}{r^2} - \frac{2}{r^2} \frac{\partial u_\theta}{\partial \theta} \right) = 0 \quad (25)$$

$$(\lambda + \mu) \frac{1}{r} \frac{\partial}{\partial \theta} \left(\frac{1}{r} \frac{\partial}{\partial r} (r u_r) + \frac{1}{r} \frac{\partial u_\theta}{\partial \theta} + \frac{\partial u_z}{\partial z} \right) + \mu \left(\frac{\partial^2 u_\theta}{\partial r^2} + \frac{1}{r} \frac{\partial u_\theta}{\partial r} + \frac{1}{r^2} \frac{\partial^2 u_\theta}{\partial \theta^2} + \frac{\partial^2 u_\theta}{\partial z^2} - \frac{u_\theta}{r^2} + \frac{2}{r^2} \frac{\partial u_r}{\partial \theta} \right) = 0 \quad (26)$$

$$(\lambda + \mu) \frac{\partial}{\partial z} \left(\frac{1}{r} \frac{\partial}{\partial r} (r u_r) + \frac{1}{r} \frac{\partial u_\theta}{\partial \theta} + \frac{\partial u_z}{\partial z} \right) + \mu \left(\frac{\partial^2 u_z}{\partial r^2} + \frac{1}{r} \frac{\partial u_z}{\partial r} + \frac{1}{r^2} \frac{\partial^2 u_z}{\partial \theta^2} + \frac{\partial^2 u_z}{\partial z^2} \right) = 0 \quad (27)$$

where u_r, u_θ, u_z are the displacements along the r, θ and z directions, respectively, while λ and μ are the Lamè's constants, defined as:

$$\lambda = \frac{\nu Y}{(1 + \nu)(1 - 2\nu)} \tag{28}$$

$$\mu = \frac{Y}{2(1 + \nu)} \tag{29}$$

where Y is the Young's modulus and ν is the Poisson's ratio of the material.

Eqs. (25)–(27) can be simplified by reasonably assuming that the actuator does not move in the θ direction and the radial and axial displacements depend only on the related coordinates r and z , respectively:

$$u_\theta = 0 \tag{30}$$

$$u_r = u_r(r) \tag{31}$$

$$u_z = u_z(z) \tag{32}$$

With these assumptions, Eq. (26) is identically null, while Eqs. (25) and (27) become:

$$\frac{d}{dr} \left(\frac{1}{r} \frac{d}{dr} (ru_r) \right) = 0 \tag{33}$$

$$\frac{d^2 u_z}{dz^2} = 0 \tag{34}$$

Eqs. (33) and (34) admit these general solutions:

$$u_r = c_1 \frac{r}{2} + c_2 \frac{1}{r} \tag{35}$$

$$\frac{du_z}{dz} = c_3 \tag{36}$$

where c_1, c_2 and c_3 are arbitrary constants.

In cylindrical coordinates, the relations between strains ($S_{rr}, S_{\theta\theta}$ and S_{zz}) and displacements are [10]:

$$S_{rr} = \frac{du_r}{dr} \tag{37}$$

$$S_{\theta\theta} = \frac{u_r}{r} + \frac{1}{r} \frac{du_\theta}{d\theta} \tag{38}$$

$$S_{zz} = \frac{du_z}{dz} \tag{39}$$

Stresses ($T_{rr}, T_{\theta\theta}$ and T_{zz}) and strains are related by means of the material constitutive equations, here represented by the Hooke's law, which can be written in terms of the Lamè's constants as follows:

$$T_{rr} = \lambda(S_{rr} + S_{\theta\theta} + S_{zz}) + 2\mu S_{rr} \tag{40}$$

$$T_{\theta\theta} = \lambda(S_{rr} + S_{\theta\theta} + S_{zz}) + 2\mu S_{\theta\theta} \tag{41}$$

$$T_{zz} = \lambda(S_{rr} + S_{\theta\theta} + S_{zz}) + 2\mu S_{zz} \tag{42}$$

By combining Eqs. (35)–(42), the expressions of the stresses become:

$$T_{rr} = (\lambda + \mu)c_1 - 2\mu \frac{c_2}{r^2} + \lambda c_3 \tag{43}$$

$$T_{\theta\theta} = (\lambda + \mu)c_1 + 2\mu \frac{c_2}{r^2} + \lambda c_3 \tag{44}$$

$$T_{zz} = \lambda c_1 + (\lambda + 2\mu)c_3 \tag{45}$$

Suitable values of the arbitrary constants c_1, c_2 and c_3 can be obtained by imposing the following boundary conditions for the stresses (tensile stresses are assumed positive):

$$T_{rr} |_{r=a} = -p_a \tag{46}$$

$$T_{rr} |_{r=b} = -p_b \tag{47}$$

$$T_{zz} = 0 \tag{48}$$

The stress along z is here assumed zero (Eq. (48)), in order to deduce the expressions of the active strains only, i.e., due to the pressures p_a and p_b only.

The conditions above originate these equations:

$$(\lambda + \mu)c_1 - 2\mu \frac{c_2}{a^2} + \lambda c_3 = -p_a \tag{49}$$

$$(\lambda + \mu)c_1 - 2\mu \frac{c_2}{b^2} + \lambda c_3 = -p_b \tag{50}$$

$$\lambda c_1 + (\lambda + 2\mu)c_3 = 0 \tag{51}$$

The solution of this system of equations for the unknown c_1, c_2 and c_3 gives:

$$c_1 = \frac{\lambda + 2\mu}{3\mu\lambda + 2\mu^2} \frac{p_b b^2 - p_a a^2}{a^2 - b^2} \tag{52}$$

$$c_2 = \frac{(p_b - p_a)a^2 b^2}{2\mu(a^2 - b^2)} \tag{53}$$

$$c_3 = -\frac{\lambda}{3\mu\lambda + 2\mu^2} \frac{p_b b^2 - p_a a^2}{a^2 - b^2} \tag{54}$$

The substitution of Eqs. (52)–(54) into Eqs. (43)–(45) provides the expressions of the stresses:

$$T_{rr} = \frac{p_b b^2 - p_a a^2}{a^2 - b^2} - \frac{(p_b - p_a)a^2 b^2}{a^2 - b^2} \frac{1}{r^2} \tag{55}$$

$$T_{\theta\theta} = \frac{p_b b^2 - p_a a^2}{a^2 - b^2} + \frac{(p_b - p_a)a^2 b^2}{a^2 - b^2} \frac{1}{r^2} \tag{56}$$

$$T_{zz} = 0 \tag{57}$$

By using the following Hooke's equations, written in terms of Y and ν ,

$$S_{rr} = \frac{1}{Y} [T_{rr} - \nu(T_{\theta\theta} + T_{zz})] \quad (58)$$

$$S_{\theta\theta} = \frac{1}{Y} [T_{\theta\theta} - \nu(T_{rr} + T_{zz})] \quad (59)$$

$$S_{zz} = \frac{1}{Y} [T_{zz} - \nu(T_{rr} + T_{\theta\theta})] \quad (60)$$

the expressions of the strains are easily obtained:

$$S_{rr} = \frac{1}{Y} \left[(1 - \nu) \frac{p_b b^2 - p_a a^2}{a^2 - b^2} - (1 + \nu) \frac{(p_b - p_a) a^2 b^2}{a^2 - b^2} \frac{1}{r^2} \right] \quad (61)$$

$$S_{\theta\theta} = \frac{1}{Y} \left[(1 - \nu) \frac{p_b b^2 - p_a a^2}{a^2 - b^2} + (1 + \nu) \frac{(p_b - p_a) a^2 b^2}{a^2 - b^2} \frac{1}{r^2} \right] \quad (62)$$

$$S_{zz} = \frac{2\nu}{Y} \frac{(p_b b^2 - p_a a^2)}{b^2 - a^2} \quad (63)$$

Eqs. (61)–(63) enable the derivation of three quantities of interest for the description of the actuator performances: the engineering strains of the working length (axial strain) and of the inner and outer radii (radial strains), defined as the percentage variation of the quantity of interest. They can be respectively calculated as:

$$\frac{\Delta L}{L} = \frac{1}{L} \int_0^L S_{zz} dz = \frac{2\nu}{Y} \frac{(p_b b^2 - p_a a^2)}{b^2 - a^2} \quad (64)$$

$$\frac{\Delta a}{a} = \frac{1}{2\pi} \int_0^{2\pi} S_{\theta\theta}(a) d\theta = \frac{1}{Y(b^2 - a^2)} \times [p_a((1 - \nu)a^2 + (1 + \nu)b^2) - 2p_b b^2] \quad (65)$$

$$\frac{\Delta b}{b} = \frac{1}{2\pi} \int_0^{2\pi} S_{\theta\theta}(b) d\theta = \frac{1}{Y(b^2 - a^2)} \times [-p_b((1 - \nu)b^2 + (1 + \nu)a^2) + 2p_a a^2] \quad (66)$$

Finally, the property of constancy of volume of the elastomer implies a value of $\nu=1/2$ for its Poisson's ratio, which gives:

$$\frac{\Delta L}{L} = \frac{p_b b^2 - p_a a^2}{Y(b^2 - a^2)} \quad (67)$$

$$\frac{\Delta a}{a} = \frac{1}{Y(b^2 - a^2)} \left[p_a \frac{a^2 + 3b^2}{2} - 2p_b b^2 \right] \quad (68)$$

$$\frac{\Delta b}{b} = \frac{1}{Y(b^2 - a^2)} \left[-p_b \frac{b^2 + 3a^2}{2} + 2p_a a^2 \right] \quad (69)$$

The substitution of Eqs. (23) and (24) into the previous equations provides the relations of the model describing the electromechanical transduction operated by the actuator.

3.3. Material characterisation

A plot of the engineering stress (force per unit unstrained cross-section) versus the engineering strain (percentage variation of the sample length), resulting from a test of passive uniaxial extension of the experimented silicone elastomer, is shown in Fig. 4. It presents the typical non-linear trend common to rubber-like materials [11]. However, in the region of small strains (separately emphasised in the same figure), the variation of the slope of the characteristic is remarkably less pronounced and the approximation of the material as a linearly elastic body, assumed in the model presented above, applies. The value of the Young's modulus around a 5% passive strain, used as prestrain in the active tests (Section 2.4), was calculated as the derivative of the curve in this point and resulted $Y=5$ MPa.

The experimental set-up used to perform the dielectric characterisation of the material (Section 2.3) permitted the measurement of the real and imaginary parts of its effective complex relative dielectric constant $\epsilon_{r,\text{eff}}^*$, defined as:

$$\epsilon_{r,\text{eff}}^* = \epsilon'_{r,\text{eff}} - j\epsilon''_{r,\text{eff}} = \epsilon'_r - j \left(\epsilon''_r + \frac{\sigma_{dc}}{\omega\epsilon_0} \right) \quad (70)$$

where $j^2=-1$, ω is the working angular frequency, ϵ'_r and ϵ''_r are the real and imaginary parts of the actual relative permittivity ϵ_r^*

$$\epsilon_r^* = \epsilon'_r - j\epsilon''_r \quad (71)$$

which quantifies the material polarisation response, while σ_{dc} is the electrical dc conductivity, which takes into account

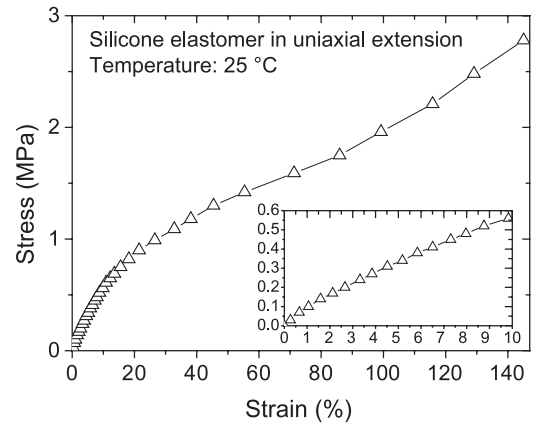


Fig. 4. Engineering stress–strain passive characteristic of the tested silicone elastomer. The first part of the plot is reported also in the included frame.

the contribution coming from free charge carriers. Recorded values of $\epsilon'_{r,eff}$ and $\epsilon''_{r,eff}$ are reported in Fig. 5.

The real part ϵ'_r of the complex constant corresponds to the relative dielectric constant ϵ_r , representing one of the input parameters for the proposed electromechanical model. The presented flat dielectric spectrum within the wide frequency range reveals a value of $\epsilon_r=3$.

As an observation, the constancy of the real part of the permittivity and the substantially null value of its imaginary part indicate that the elastomer behaves like a perfect electrical insulator in the experimented frequency range, owing to the absence of dissipative effects related to both polarisation or charge carrier migration.

3.4. Experimental validation of the model

Fig. 6 presents measured and predicted values of the axial strain of the silicone-made actuator for different applied voltages per unit wall thickness.

Voltage per unit thickness cannot be regarded here as an electric field, even though it has the same dimensions, since for a cylindrical capacitor, the electric field between the electrodes varies radially as the inverse of the radial coordinate.

The theoretical curve, derived from the proposed model, fits well the experimental data plot. This curve was obtained from the combination of Eqs. (23), (24), and (67), and it has this quadratic expression:

$$\frac{\Delta L}{L} = \beta \left(\frac{V}{b-a} \right)^2 \quad (72)$$

where the coefficient β , calculated from the reported values of a , b , Y and ϵ_r (Sections 2.4 and 3.3), resulted $\beta=3.75 \times 10^{-6} \mu\text{m}^2/\text{V}^2$.

As an observation, we stress that the applied high voltages, required by the relatively high wall thickness of the tube and withstood by the silicone high dielectric strength, did not cause dielectric breakdown of the material. In fact, the increase of the driving voltage was operated only up to the

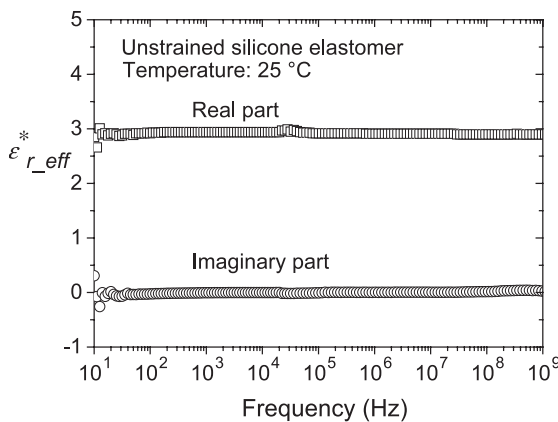


Fig. 5. Frequency dependence of the real and imaginary parts of the effective relative permittivity of the tested silicone elastomer.

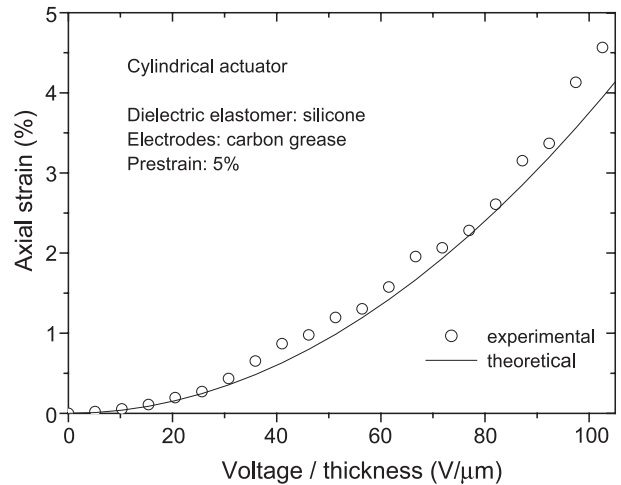


Fig. 6. Experimental and theoretical axial strain versus applied voltage per unit wall thickness for a realised actuator.

limiting value imposed by the dielectric breakdown of the air surrounding the electrodes outside the polymer. Consequently, it can be deduced that the material could show strains potentially higher than the maximum value actually recorded in this study. However, the experimental testing of the device was here aimed only at a validation of the proposed model and the explored operative range (0–100 V/μm) was considered sufficient for such a purpose.

4. Conclusions

An electromechanical model of a dielectric elastomer cylindrical actuator was formulated by means of independent electrical and mechanical analyses of the device configuration.

The proposed model permitted to analytically describe and accurately predict the functioning of a low-prestrained silicone-made actuator having carbon grease electrodes, as demonstrated by the good agreement between expected and measured axial strains within the tested voltage range.

Application-oriented design of cylindrical actuators made of dielectric elastomers would benefit from future extensions of the proposed electromechanical model to high-prestrain ranges, where material non-linearities have to be taken into account to fully describe the actuating capabilities of these devices.

Acknowledgements

Authors acknowledge Dr. med. Rolf Siegel, from Bionic Surfaces, Germany, who supplied the silicone tubing used as dielectric material, and Dr. Giuseppe Gallone, from University of Pisa, who performed the dielectric constant measurements.

References

- [1] R.E. Pelrine, R.D. Kornbluh, J.P. Joseph, Electrostriction of polymer dielectrics with compliant electrodes as a means of actuation, *Sensors and Actuators A* 64 (1998) 77–85.
- [2] R. Heydt, R. Kornbluh, R. Pelrine, V. Mason, Design and performance of an electrostrictive-polymer-film acoustic actuator, *Journal of Sound and Vibration* 215 (2) (1998) 297–311.
- [3] R. Pelrine, R. Kornbluh, J. Joseph, R. Heydt, Q. Pei, S. Chiba, High-field deformation of elastomeric dielectrics for actuators, *Materials Science and Engineering C* 11 (2000) 89–100.
- [4] R. Pelrine, R. Kornbluh, Q. Pei, J. Joseph, High-speed electrically actuated elastomers with strain greater than 100%, *Science* 287 (2000) 836–839.
- [5] Q. Pei, R. Pelrine, S. Stanford, R. Kornbluh, M. Rosenthal, Electro-elastomer rolls and their application for biomimetic walking robots, *Synthetic Metals* 135–136 (2003) 129–131.
- [6] F. Carpi, P. Chiarelli, A. Mazzoldi, D. De Rossi, Electromechanical characterisation of dielectric elastomer planar actuators: comparative evaluation of different electrode materials and different counterloads, *Sensors and Actuators A* 107 (2003) 85–95.
- [7] R. Pelster, A novel analytic method for the broadband determination of electromagnetic impedances and material parameters, *IEEE Transactions on Microwave Theory and Techniques* 43 (7) (1995) 1494–1501.
- [8] L.R.G. Treloar, *The Physics of Rubber Elasticity*, Third edition, Clarendon Press, Oxford, 1975, p. 61.
- [9] J.H. Heinbockel, *Introduction to Tensor Calculus and Continuum Mechanics*, Old Dominion University, Norfolk-Virginia, 1996, pp. 255–257.
- [10] S.P. Timoshenko, *Theory of Elasticity*, Third edition, International Student Edition, McGraw-Hill press, Singapore, 1982, p. 76.
- [11] L.R.G. Treloar, *The Physics of Rubber Elasticity*, Third edition, Clarendon Press, Oxford, 1975, p. 2.